The functional architecture of skeletal compared to cardiac musculature; myocyte orientation, lamellar unit morphology, and the helical ventricular myocardial band.

Abstract

How the cardiomyocytes are aggregated within the heart walls remains contentious. We still do not fully understand how the end-to-end longitudinal myocytic chains are arranged, nor the true extent and shape of the lamellar units they aggregate to form. In this review, we show that an understanding of the complex arrangement of cardiomyocytes requires knowledge of 3-dimensional cell orientation (helical and intrusion angle), and appreciation of cell packing within the connective tissue matrix. We show how visualisation and segmentation of high resolution 3-dimensional image data can accurately identify the morphology and orientation of the myocytic chains, and the lamellar units. Some maintain that the ventricles can be unwrapped in the form of a "helical ventricular myocardial band". Implying the ventricular muscle is arranged comparable to that of skeletal muscles, in an ordered fashion, as a compartmentalised band with selective regional innervation and deformation, and a defined origin and insertion. In contrast to the simpler interpretation of the helical ventricular myocardial band, we provide insight as to how the complex myocytic chains, the heterogeneous lamellar units, and connective tissue matrix form an interconnected meshwork, which facilitates the complex internal deformations of the ventricular wall. We highlight the dangers of disregarding the intruding cardiomyocytes. Preparation of the band destroys intruding myocytic chains, and thus disregards the functional implications of the antagonistic auxotonic forces they produce. We conclude that the ventricular myocardium is not analogous to skeletal muscle, but is a complex 3-dimensional meshwork, with a heterogeneous branching lamellar architecture.

Key words: cardiac muscle; myocyte orientation; lamellar units; 3-dimensional meshwork.

Introduction

The manner in which the cardiomyocytes are aggregated within the walls of the heart remains contentious. We still do not fully understand how the end-to-end longitudinal chains of cells are arranged, nor the true extent and shape of the higher order aggregations they form collectively. This is surprising, since it is now more than 150 years since Pettigrew emphasised that although, like skeletal muscles, the walls of the heart are made up of striated muscle cells, in contrast to skeletal muscles, "the fibres of the ventricles, as a rule, have neither origin nor insertion, i.e. they are continuous alike at the apex of the ventricles and at the base" (Pettigrew, 1864). He was making an analogy with involuntary smooth muscles, which are often arranged in continuous circular structures such as in the urinary bladder, the uterus, or the walls of the arterioles. It is important that we understand what Pettigrew, and others since who have used a peeling method to deconstruct the heart (Greenbaum et al., 1981), meant by "fibres". Certainly, they did not mean fibres in the sense of single cells, as the term is used in skeletal muscle. The cardiomyocytes, the individual contractile cells of the ventricles, are typically only a tenth of a millimetre long (Satoh et al., 1996). Those describing "fibres" in heart muscle, therefore, generally mean multicellular longitudinally aggregated structures that have a visually distinct preferred direction, and that tend to separate as a strip from the remaining tissue when progressively peeled away. Others have described collective aggregates of cardiomyocyte "fibres" that can be identified by their perimysial boundaries. These so-called lamellar units are displayed clearly after pneumatic distension of cardiac tissue (Lunkenheimer and Niederer, 2012). Caution is needed, however, when interpreting transverse sections of the heart wall, because the cleavage planes between these aggregates give the impression of "fibre-like" structures with a preferred direction. This does not, necessarily, reflect the orientation of the cardiomyocytes themselves. As we shall show, this can be misleading. The apparent preferred direction may reflect the short axis of a lamellar unit, and thus be near orthogonal to the true direction of the cardiomyocytes, emphasising the need for care in the interpretation of images of the microstructure of the heart.

Following his many dissections, Pettigrew considered that it was possible to subdivide the wall of the left ventricle into 7 layers. He also acknowledged, nonetheless, that the cardiomyocyte chains "…are further distinguished by the almost total absence of cellular tissue as a connecting medium – the fibres being held together partly by splitting up and running into each other, and partly by the minute ramifications of the cardiac vessels and nerves." (Pettigrew, 1864). He understood, therefore, that there is no anatomically distinct substructure that makes up the ventricular musculature, and that the layers he described are intimately connected with one another in multiple directions, including the radial direction. Many anatomists and physiologists have studied the fine structure of both cardiac and skeletal muscle in the 155 years subsequent to the description provided by Pettigrew. Some investigators, for example, maintain that the ventricular mass can be unwrapped in the form of a "helical ventricular myocardial band" (Buckberg, 2005) (Fig. 1). This suggestion is based on the concept initially expounded by Torrent-Guasp, namely that chains of cardiomyocytes take their origin from the pulmonary trunk, and can be followed throughout the entire cardiac mass before eventually inserting into the aortic root (Fig. 1). This implies that the muscle of the ventricular cone is arranged in an ordered fashion comparable to many skeletal muscles, with a defined origin and insertion (Torrent-Guasp, 1957; Torrent-Guasp et al., 2005). Others, in contrast, have illustrated the cardiomyocytes aggregated together in lamellar fashion, that is, in thin sheets, showing in their diagrams stacked layers of aggregated cardiomyocytes separated by fibrous shelves extending transmurally, from epicardium to endocardium across the ventricular wall (LeGrice et al., 1995a). An elegant subsequent investigation from this group, which used confocal microscopy to illustrate the architectural arrangement, showed that the notion of transmural sheets was, in fact, an exaggeration of the true anatomy (Pope et al., 2008). The patterns of the aggregations revealed by the confocal study are more in keeping with the notion of a three-dimensional meshwork. This was the concept described by some of the current authors in a previous contribution to "Clinical Anatomy", (Anderson et al., 2009a), although without emphasis on the lamellar architecture, which we will discuss below.

An understanding of the complex arrangement of cardiomyocytes within the walls of the heart however, requires not only knowledge of the muscle cells themselves, but also an appreciation of the precise manner of their packing within the supporting connective tissue matrix. In this respect, Borg and Caulfield showed that, as with the skeletal muscles, the supporting fibrous tissue of the heart could be analysed in terms of its endomysial and perimysial components (Borg and Caulfield, 1981). In this review, we show how attention to the way the matrix packs together individual cells, and attaches them to their neighbours to form higher order aggregates, provides an understanding of the similarities, but more importantly the differences, in the architecture of the skeletal as opposed to the cardiac musculature. Furthermore, we show how visualisation and segmentation of 3-dimensional image data can identify the morphology and orientation of the cardiomyocytes, and the lamellar units they form (Figs. 2-3). We thus provide insight as to how these heterogeneous structures, which allow shearing while maintaining connections with their neighbours, act to produce the complex internal deformations of the ventricular wall, and do not support the simpler interpretation of a helical ventricular myocardial band. We define these aggregates by our ability to follow them as closely-assembled groups of cardiomyocytes, separated from neighbouring aggregates by extracellular matrix and space, or by their abutment with other aggregates that have a clearly different average orientation. We note that this virtual dissection is only possible in datasets that have sufficient spatial resolution to allow one to observe the boundaries between individual cardiomyocytes.

The arrangement of the skeletal myocytes

Activation

Skeletal muscles are voluntary, and are activated via their motor endplates. The most fundamental difference between cardiac and skeletal muscle is that cardiac muscle functions as a syncytium; in every cardiac cycle there is contraction of all of the cardiomyocytes. To achieve this, cells communicate one with the other via electrically conducting gap junctions, allowing a coordinated wave of depolarisation, triggered in the sinus node, to spread over and through the entire atrial and ventricular myocardium. Muscular pumping effort is controlled by variation in the amount of force produced by the individual cardiomyocytes, which itself depends on preload, afterload and sympathetic stimulation, and not by recruiting more or less individual motor units, as is the case in skeletal muscle. In skeletal muscle, the muscle cells are not electrically connected to one another. Each cell is supplied with a nerve ending. When fibres are stimulated to contract by the arrival of an action potential at their motor end plate, that contraction does not induce contractile activity in their immediate neighbours. Control of force in skeletal muscle can thus be achieved by recruitment of more or less motor units as appropriate by the central nervous system. A motor unit is the population of muscle fibres innervated by one motorneuron via its multiple terminal branches. A typical skeletal muscle in a human limb has a few hundred motor units. This gives skeletal muscle the very large dynamic range of force output required for fine and precise movement at one extreme, and gross powerful force production at the other.

Structure

Skeletal muscles take various forms, but they all possess identifiable external origins and insertions. Apart from the tongue and the uvula, these origins, themselves formed from specialised areas of collagen, are typically attached to bony structures, and the insertions are via specialised tendinous entities, which also usually insert to bony structures. The tongue and uvula are worthy of special

attention, because the arrangement of their myocytes has been considered as closely analogous to those in ventricular myocardium; we consider this analogy below.

Single skeletal myocytes may extend over many centimetres from origin to insertion. The word “fibre” is thus suitable to describe single skeletal myocytes. Such individual cells can be dissected from small muscles as intact single fibres, and are commonly used in physiological testing. The single skeletal muscle cell is thus able to perform the function of the whole muscle: that is, to generate a longitudinal contractile force between two points. This is not the case for an individual cardiac muscle cell. It cannot generate a pressurising force upon an enclosed fluid, as is needed for normal systolic pump function. The longitudinal strain created collectively by all the cardiomyocytes only equates to ~15% shortening (Lehto and Tirri, 1980; Rodriguez et al., 1992) systolic strains in the left ventricle, however, can greatly exceed this value (Arts et al., 1984; Arts et al., 1979). Shortening of a cardiomyocyte causes only an 8% increase in its diameter, which does not explain the 40% radial wall thickening and ~60% ejection fraction in systole (Arts et al., 1979). It is the complex 3-dimensional arrangement of the myocardial mesh, made up of the cardiomyocytes and their supporting connective tissue, which that permits greater deformation than its active constituents. It is the nature of this cellular arrangement that has fascinated students of the heart for decades.

Skeletal myodynamics

Although individual skeletal muscle cells can generate force between two points, they are collected together into larger functional populations, which we call fascicles. Multiple fascicles make up a single skeletal muscle. Such muscles have a characteristic supporting fibrous matrix that extends from origin to insertion. It is made up of the epimysium, which covers the whole muscle; the perimysium, which divides the muscle into fascicles or bundles of typically a few hundred myocytes; and the endomysium, which provides a thin sheath around each individual myocyte. These progressively more delicate sheaths also provide the tracts along which the intramuscular neural and vascular networks find their

way to individual muscle fibres. There is a large amount of literature on the function of these connective tissue layers in transmitting tension from one fibre to its neighbour (Huijing, 1999). Some skeletal muscle fibres do not run all the way from origin to insertion. The force generated by such fibres is transmitted laterally to the endomysial and perimysial network, which then transmits the shortening force to the muscle insertion. The mechanism and cellular machinery underlying such lateral transmission of force is the subject of ongoing research (Ramaswamy et al., 2011; Street, 1983).

The overall arrangement of myocytes in skeletal muscles, therefore, is well established. The fibres are packed in bundles, but contract as individual units to pass their generated force ultimately to the insertion of the muscle. A commonly cited deviation from this generalisation is the muscle of the tongue. In this case, there is a mixture of extrinsic muscles, which are connected to bony origins, and intrinsic muscles, which have no bony origin (Kier and Smith, 1985). The intrinsic muscles interweave, so that in cross sections of the tongue, bundles can be seen running orthogonally to one another (Fig. 4), and this has triggered comparison with the changing direction of myocyte orientation across the heart walls (Streeter and Bassett, 1966; Streeter et al., 1969).

It is the interaction between the antagonistic forces generated by these orthogonal bundles that allows the remarkable freedom of movement of the free portion of the tongue, which underscores both speech and swallowing. It also explains how linear contraction of opposing bundles can be integrated into curling or bulging actions. This is surely instructive as to the action of the heart walls, as the heart is indeed capable of producing antagonistic forces locally within its walls (Lunkenheimer et al., 2004). The heart, however, does not show such a clear separation of opposing bundles as in the tongue. Rather, the transformations between one primary cell direction and another is achieved more gradually, with the subtle changes at increasing depths within the walls producing the so-called helical angle (Streeter and Bassett, 1966; Streeter et al., 1969) (Fig. 5). Sharp delineations between populations of cardiomyocytes running in one direction, and neighbouring populations running orthogonally,

therefore, is unusual. Such an arrangement is found, however, in the tongue (Fig. 4), and in the muscular tentacles of the squid and octopus, and in the trunk of the elephant (Kier and Smith, 1985).

Comparison with the heart

As we will demonstrate, the precise packing of cardiomyocytes within the heart walls is worthy of careful study. Many students of the heart have recognised that the spiral or helical arrangement of cellular aggregates within the heart wall means that torsional forces, as well as compressive forces, must be generated, and that shear forces must exist between cardiomyocytic chains, and between lamellar units, as they shorten and deform (Ingels, 1997; Lunkenheimer et al., 2004; Smerup et al., 2013b). It has been suggested that the arrangement of the connective tissues between lamellar units forms planes along which groups of cells can slide relative to one another, so-called shearing (LeGrice et al., 1995b). Such spaces have been identified as 'cleavage planes' in scanning electron micrographs of cardiac tissue (LeGrice et al., 1995a; Lunkenheimer and Niederer, 2012), but the nature of the technique means that only very small samples of issue can be studied. Histological analysis is difficult because, as our recent micro-computed tomography analysis demonstrates (Fig. 5), the primary direction of the cardiomyocytes changes almost continuously, and thus a 2-dimensional section cannot illustrate the 3-dimensional 'bundling' or aggregation of cardiomyocytes. Furthermore, the primary direction of chains of cardiomyocytes may not be tangential to the near-circular cross section of the left ventricle. Both the purported "helical ventricular myocardial band" (Fig. 1), and the earlier loops described by Pettigrew, were envisaged as encircling the ventricular cone in a direction parallel to the epicardial surface. We now know that some aggregates of cardiomyocytes have a primary direction that includes a transmural component, 'intruding' from epicardium to endocardium (Lunkenheimer et al., 2013; Schmid et al., 2007; Smerup et al., 2013a) (Figs. 5-6). Figure 5 shows the complex meshwork of myocytes in a small segment of the left ventricular posterior wall, myocyte orientation maps are generated by eigen-analysis (Zhao et al., 2012) of micro-computed tomographic data with a spatial resolution of 20 μm. Although the helical angles found in the mid-wall suggest predominantly circumferential tangentially orientated

cells, the corresponding intruding angle is complex. This supports the notion of a complex cardiac mesh, and highlights the necessity to investigate the microanatomy of the heart in 3-dimensions. A 3-dimensional technique is, therefore, essential in order to distinguish between one cellular chain and another. With this in mind, we have utilised the preferential uptake of iodine by the myocytes compared to connective tissue to resolve individual myocytes and their aggregates using micro-computed tomography (Jeffery et al., 2011; Stephenson et al., 2012) (Figs. 2-3). This makes it possible to identify aggregates of cells that are separated from their neighbours by extracellular space or the presence of connective tissue. The lamellar units can now, therefore, be followed through the ventricular mass (Fig. 3). The regional variation among these structures, and their typical shapes and defining characteristics, will be published as we perform further analysis (Stephenson et al. unpublished data). We will return to the fine scale packing of the ventricular cardiomyocytes when we have considered two examples in which the separation of structural components of the heart may be clearly identified.

The cardiac conduction system

In one particular case, distinct aggregations of specialised cardiomyocytes can be identified, separated from the working myocardium by connective tissue structures. These are the populations of cells making up the cardiac conduction system (Fig. 7). We have already emphasised the obvious fundamental difference between the cardiomyocyte and the skeletal myocyte, namely that the muscle cells within the heart are not under voluntary control. Thus, they lack motor end plates. They are, nonetheless, excitable. Activation is provided by small collections of specialised cardiomyocytes, which collectively form the cardiac conduction system (Anderson et al, 2009b). In fact, all of the cardiomyocytes conduct, but the so-called “specialised system” is responsible for generation and propagation of myocardial excitation. The cardiomyocytes that generate the cardiac impulse, the so-called ‘pacemaker’, are grouped together within the sinus node. The shape of the sinus node varies between species. The term node suggests a small collection of cells, this is misleading. In some species, 3-dimensional analysis has shown it to be a heterogeneous streak of cells, spanning the intercaval region

to varying degrees (Dobrzynski et al., 2005; Liu et al., 2007; Stephenson et al., 2012) (Fig.8). The node-like arrangement, however, is more justifiable when considering the arrangement found in the human heart (Anderson and Ho, 1998). At the borders of the node, the nodal cardiomyocytes are in direct continuity with the working cardiomyocytes of the atrial walls. The nodal cells and the working cardiomyocytes can be distinguished on the basis of the connexins found within the intercalated discs joining adjacent cells (Dobrzynski et al., 2013). Those of the sinus node, which are slowly conducting, are abundant in connexin 40, while those of the working cardiomyocytes are abundant in connexin 43. The nodal cells can also be distinguished by their content of HCN4, the protein that allows the so-called "funny current", which makes the nodal cells intrinsically rhythmical (Chandler et al., 2009) It is the impulse generated by the specialised cardiomyocytes within the sinus node that drives the working cardiomyocytes packed together within the atrial walls. For a comprehensive review of connexin distribution across the working myocardium and specialised tissues see Dobrzynski et al. (2013).

All of the atrial cardiomyocytes are able to conduct the cardiac impulse, since they are linked together within a functional syncytium, although each cardiomyocyte is an individual entity. The junctions between adjacent myocytes through the intercalated discs, which contain connexin 43, serve to conduct the sinus impulse rapidly towards the atrioventricular junction (Dobrzynski et al., 2013). At the same time, the activation of the cardiomyocytes packed together within the atrial walls provides atrial systole, propelling the blood into the ventricular chambers. The atrioventricular node, like the sinus node, is a collection of histologically specialised cardiomyocytes (Anderson and Ho, 1998). It has the function of slowing the atrial impulse subsequent to atrial contraction, so that the nodal delay permits the ventricles to fill during the diastolic phase of the cardiac cycle. Therefore, while much has been written concerning the possible existence of tracts of specialised cardiomyocytes extending from the sinus node to the atrioventricular node (Anderson and Ho, 1998; James, 1963), a case can be marshalled against this on simply teleological grounds, since there is no need for such tracts. Histological examination of the internodal atrial working myocardium in most species also fails to reveal tracts of cardiomyocytes that are insulated from their neighbours (Anderson et al., 2009b). But this structural phenomenon is yet

to be explored in all species using high-resolution 3-dimensional imaging techniques such as micro-computed tomography.

A potential exception to this rule, however, is found in the rabbit heart. In this species, insulated bundles of cardiomyocytes are present at the attachments of the valves of the systemic venous sinus. Known as the sinuatrial ring bundle (Bojsen-Moller and Tranum-Jensen, 1972), this insulated tract does extend between the locations of the sinus and the atrioventricular nodes. But despite the fact that its cardiomyocytes are joined together by gap junctions containing connexin 43, electrophysiological studies have shown the cells within the tract to be slowly conducting (Hiraoka and Sano, 1976). Evidence is also lacking thus far that the cells within the insulated tract possess direct connections with the cardiomyocytes making up the sinus and atrioventricular nodes. The presence of the ring bundle, therefore, does serve to demonstrate that, in certain species, the cardiomyocytes can be aggregated together to form muscular structures that are discrete from the remainder of the cardiac walls.

An additional arrangement of cardiomyocytes aggregated together to produce an unequivocal tract is to be found in the atrioventricular conduction axis (Tawara, 2000) (Fig. 9). This pathway originates in the atrioventricular node, where the nodal cardiomyocytes are in direct communication with the atrial working cardiomyocytes through zones of transitional cells (Li et al., 2008). The nodal cardiomyocytes, when traced distally, aggregate together and enter the insulating tissues of the atrioventricular junctions, as the penetrating bundle (Fig. 9A,C). Within the insulating tissues, the anterior aspect of the axis is known as the bundle of His (Fig. 9B,D). Having entered the ventricles, the axis divides to form bundles insulated by fibrous sheets from the adjacent myocardium. These fascicles run on either side of the ventricular septum, and are known as the ventricular bundle branches (Fig. 9B,D). These branches are continuous with the Purkinje fibre network, a complex branching web of longitudinal chains of specialised myocytes with free running aspects, responsible for coordinated contraction of the ventricles (Ansari et al., 1999; Eliška, 2006; Stephenson et al., 2012) (Fig. 7). Like the sinuatrial ring bundle in the rabbit, therefore, the atrioventricular conduction axis exemplifies an isolated system of

cardiomyocytes that is insulated from the overall mass of working cardiomyocytes, and which can be recognised as an anatomically discrete entity.

The atrioventricular structures

By virtue of the insulating nature of the tissues of the atrioventricular grooves, the cardiomyocytes packed together within the atrial and ventricular walls constitute separate working units. Much has been written regarding the presence of a "fibrous skeleton" within these grooves. In fact, the necessary insulation between the atrial and ventricular muscle masses is largely provided by the fibro-adipose tissues gathered together within the grooves (Dean et al., 1994). Collagenous cords can be found within the inferior and leftward part of the atrioventricular junctions supporting the mural leaflet of the mitral valve, but it is rare to find complete "skeletal" elements supporting the entirety of the mitral valvar leaflet. Bony elements exist in the large hearts of some bovine species (James, 1965), and cartilage is to be found in other species, such as the otter (Egerbacher et al., 2000). Even in these species, however, the structures do not provide "skeletal" support for the cardiomyocytes. A major difference between cardiomyocytes and skeletal myocytes, therefore, is that cardiomyocytes cannot be recognised to have "skeletal" support, not even from the leaflets of the cardiac valves. On the contrary, it is the leaflets of the atrioventricular valves, which are suspended from the cardiac junctions. At the ventriculo-arterial junctions, the semilunar hinges of the arterial valvar leaflets are attached as much to arterial as to muscular structures (Dean et al., 1994). The strongest part of the alleged fibrous skeleton is produced in the regions of continuity between the leaflets of the aortic and atrioventricular valves. The larger part of the aortic valvar orifice, however, has no contact with the ventricular musculature, since its non-adjacent and left coronary aortic leaflets are in fibrous continuity with the aortic leaflet of the mitral valve (Anderson et al., 1991). There has been confusion as to whether the musculature of left ventricle forms an insertion at the aortic root, as is postulated by those who promote the notion of a "helical ventricular myocardial band" (Torrent-Guasp, 1957) (Fig. 1).

The Cardiomyocytes

The cardiomyocytes, therefore, unlike skeletal muscles, do not have discrete origins and insertions. Instead, each cardiomyocyte is linked to its neighbours, as is the case for smooth muscle. The cardiomyocytes, nonetheless, do share with skeletal myocytes their striated appearance. This is because, as is also the case for skeletal myocytes, their basic working unit is the sarcomere. Numerous sarcomeres are aligned end-to-end within the typical working cardiomyocyte. Unlike the skeletal myocytes, however, each cardiomyocyte is joined to several of its neighbours, by end-to-end connections and side branches (Barnett and Iaizzo, 2009). The major union between adjacent cardiomyocytes is at their ends, so that there is formation of endless chains, which extend throughout the atrial and ventricular walls respectively. The alignment of the cells in this fashion produces an obvious “grain” (Greenbaum et al., 1981), again evident in the walls of both the atrial and ventricular chambers and confirmed by histological analysis (Streeter and Bassett, 1966) and analysis of cell orientation by algorithmic computation of attenuation data in 3-dimensional micro-computed tomographic datasets (Aslanidi et al., 2012; Haibo et al., 2013) (Figs. 5,6,10). It is the increased conduction velocity of the wave of depolarisation *along* this ‘grain’, rather than *across* it, that produces differential rates of conduction throughout the heart. This is observed most notably within the atrial walls, with faster conduction observed along muscle bundles, such as the pectinate muscles and Bachman’s bundle.

The Architecture of the Cardiac Walls

The nature of packing together of the cardiomyocytes within the cardiac walls reveals significant architectural differences between the atrial and ventricular chambers. An obvious gross hierarchical pattern can be discerned within the walls of the atrial appendages, with groups of cardiomyocytes aggregated together to form the pectinate muscles. Analysis of micro-computed tomographic data confirms that, in such bundles, the cardiomyocyte orientation is generally along the long axis. An analogous structure can be seen in the endocardial trabeculations of the ventricles. Figure 5 shows a

trabeculation with cardiomyocytes running vertically, as denoted by a high helical angle (red), and low intrusion angle (green). The cardiomyocytes are similarly aggregated in parallel fashion in the prominent bundles forming the rims of the atrial septum, Bachmann's bundle, within the terminal crest, and in the different layerings present within the thicker walls of the left atrium (Sanchez-Quintana et al., 2013). The situation is much less clear-cut with regard to the architecture of the ventricular walls.

The obvious patterns or 'grain' that reflect the long axes of the chains of aggregated cardiomyocytes have been recognised for centuries. The spiralling configurations to be found at differing depths within the ventricular walls was described in great detail by Pettigrew (Pettigrew, 1864). He described the opposing helical grain in the endocardial and epicardial layers, along with a circumferential central layer. He also emphasised the opposing spirals to be found at the ventricular apex. Pettigrew (1864), nonetheless, was well aware that the change in grain did not reflect the presence of individual muscles within the overall ventricular cone. He noted the relative uniformity of the walls.

The notion that the ventricular cone could be divided into a few subunits stems from the account of Mall (1911), who described entities such as the deep sinospiral muscle (Mall, 1911). Lev and Simkins (1956) then countered that such tracts could be manufactured at the whim of the dissector (Lev and Simkins, 1956). They recapitulated the diktat of Pettigrew, namely that the heart was not to be analysed as similar to skeletal muscle. These caveats had no influence on the interpretations of Torrent-Guasp. He was able to unwrap the ventricular cone in the form of a continuous strip extending from the aortic root to the pulmonary infundibulum (Torrent-Guasp, 1957). His dissections, of necessity, transected the multiple connections between the parts of the band, including radially intruding myocytic chains, which are found at the alleged boundaries of the band. The obvious spiralling to be seen within the purported band, nonetheless, has proved influential in persuading others of the functional importance of the concept (Buckberg, 2005). Thus, the concept of the purported band has been accepted enthusiastically by some surgeons, who noted the spiralling action of the ventricular cone during their operative procedures. It also provided a seemingly robust explanation for the motions observed by

echocardiographers using speckle tracking (Buckberg et al., 2008). The spiralling nature of the tracks that can be demonstrated using diffusion tensor magnetic resonance imaging have also been cited as providing evidence for existence of the helical ventricular myocardial band (Buckberg et al., 2008). As we will show, the spiralling of the chains of cardiomyocytes demonstrated initially by Pettigrew, (Pettigrew, 1864), and endorsed by measurements of histological sections by workers such as Streeter and Bassett (1966), and Greenbaum and associates (1981), provides much better agreement with recent findings produced using diffusion tensor magnetic resonance imaging and micro-computed tomography.

Imaging the Ventricular Components

As we have discussed above, the micro-architecture of the myocardial mass has previously been investigated using dissection (Pettigrew, 1864; Lev and Simkins, 1956) or histology (Streeter and Bassett, 1966; Greenbaum et al., 1981). Over recent decades, various non-invasive techniques have gained increasing usage, particularly diffusion tensor magnetic resonance imaging, which has been widely used to elucidate the course of the aggregated chains of myocytes in both skeletal (Froeling et al., 2015) and cardiac muscles (Smerup et al., 2009). Newer techniques, such as micro-computed tomography (Haibo et al., 2013), and high-resolution magnetic resonance imaging (Gilbert et al., 2012a) have also shown promising results in assessing the complex three-dimensional structure of the myocardium, and as shown, we have ourselves used micro-computed tomography. All of these techniques are non-invasive, and make use of so-called tensors. It is worthwhile, therefore, to comment on the bases of the concepts underscoring these approaches, and emphasising their strengths and weaknesses. A tensor is a three-dimensional ellipsoidal mathematical construct calculated on a voxel-by-voxel basis, with its orientation and shape based on the local micro-anatomy. Such tensors can be calculated from the spontaneous diffusion of protons as in diffusion tensor magnetic resonance imaging, or from grayscale intensities derived from x-ray attenuation by actual structures as in micro-computed tomography. The interested reader is encouraged to consult dedicated literature in this matter. From the

tensors, it is possible to determine the longitudinal orientation of the cardiomyocytes (Smerup et al., 2013a; Smerup et al., 2009). Such investigations have produced fairly good agreement with the more traditional methods (Gilbert et al., 2012b; Holmes et al., 2000; Hsu et al., 1998). When seeking to assess the extent to which cardiomyocytes are aggregated into secondary structures, such as lamellar units or sheets, the situation becomes more complicated. A tensor in skeletal muscle will assume the shape of a bi-axial ellipsoid, which is symmetrical around its long axis. This is due to the fact that, as we have shown, no particular anatomical substructures of aggregated myocytes are to be found in skeletal muscle. Because of this, diffusion tensor magnetic resonance imaging of skeletal muscle demonstrated the myocytic architecture in terms of the longitudinal orientation of the myocytes themselves. In the myocardium, however, the tensors assume the shape of a tri-axial ellipsoid akin to a flattened American football. This, in itself, is indicative of the presence of a higher order or substructure within the anatomical arrangement of the cardiomyocytes (Kung et al., 2011). The orientation of these substructures, the so-called lamellar units or sheets, can be assessed by quantifying the angles between the eigenvectors of the tensors, and relating these to the planes or directions of the ventricular mass. A significant limitation in the assessment of the orientation of the aggregations of cardiomyocytes, however, is that techniques based on evaluation of tensors are only able to assess orientations relative to the primary eigenvectors. It is not possible using tensor imaging, therefore, to draw conclusions concerning the shape and physical extent of the myocardial aggregates. Micro-computed tomographic data, in contrast, provides information on actual physical structure, and at high resolution can resolve individual myocytes, and the higher order lamellar unit structure (Figs. 2-3). These considerations all highlight the issue of insufficient resolution in morphological analysis of cardiac micro-anatomy. Imaging techniques, which produce matrices made up of voxels, such as computed tomography and magnetic resonance imaging, can provide misleading information. Investigators should always be aware of the structures contained within their voxels below the spatial resolution of their image.

Problems with the notion of a helical ventricular myocardial band

Comparison of the architecture of skeletal and cardiac muscle provides multiple reasons why the notion of the helical ventricular myocardial band lacks anatomical foundation. It is the epimysial coverings of skeletal muscles, apart from the intrinsic muscles of the tongue and the uvula, which separate the contractile components, permitting the individual muscles to contract in independent fashion. Even within the tongue, and analogous structures such as the tentacles of squid and the trunk of the elephant, there are clear boundaries between the bundles that have a near uniform fibre orientation. In the human tongue the median, paramedian and lateral connective tissue septa are described clearly as a flexible framework giving attachment to the intrinsic muscles (Abd-el-Malek, 1939).

Innervation of muscle

Within the tongue itself, it is then the patterns of innervation that permit the longitudinal and transverse muscles to work independently. The same applies to the uvula, which is shortened by the force of its longitudinal muscles, and lengthened by the force of the wrapping circumferential compartment. The extraordinary flexibility of movement that such an arrangement affords is well understood in terms of the muscular hydrostat (Kier and Smith, 1985), in which the constituent muscles reduce one dimension of an enclosed fixed volume by their active contraction, thereby causing an increase in another dimension. The amazing flexibility of the octopus tentacle is also achieved by such means, and by a highly segmented innervation of the constituent muscles so that bending and stiffening can be achieved with no apparent restriction to any anatomical reference plane. Due to the syncytial nature of the myocardium, and the lack of dense, boundary forming, perimysial networks as found in in skeletal muscle, this selective innovation of compartmentalised muscle regions does not occur in the heart.

Functional interpretations of the helical ventricular myocardial band looks to describe cardiac contraction based on innervation and deformation of distinct bands of muscle at specific points in the cardiac cycle. But the continuous transmural arrangement of myocytes, and the interconnected branched lamellar units they form (Figs. 2-3,5), means the notion of the band disregards the multi-dimension strain the heart is capable of producing. The ability of helical muscle bundles to generate torsional,

lengthening, and shortening forces in multiple directions is discussed by Kier and Smith, and it is surprising that the principles of the muscular hydrostat have not been much applied to the function of the heart. The function of the heart as a pump is based simply on the cyclical change in the endocardial surface, and the action of the valves. The volumes of muscles are almost constant during contraction and relaxation. The total volume of the heart, therefore, changes as a function of the enclosed volume of blood (Carlsson et al., 2004). The mean mural thickening of ~40% in systole is focused by deformation of the ventricular tissue into the lumen, to generate a variation in ventricular luminal volume of approximately 60%. The reduction of the internal diameter of muscle-enclosed spaces has been discussed previously (Smerup et al., 2013b), and reaches its most obvious application in the muscle sphincters whose function is to obliterate a lumen (Russold et al., 2010).

The origin and insertion debate

Supporters of the helical ventricular myocardial band suggest the ventricular muscle has an origin at the pulmonary trunk and insertion at the aortic root (Fig. 1). As described above in the section 'atrioventricular structures', this is anatomically unfounded. Descriptions of the band suggest the 'origin' and 'insertion' are anatomically separate. Diffusion tractography achieved using diffusion tensor magnetic resonance imaging suggests this is again an oversimplification (Fig. 10). The upper panels in Figure 10 (A,B) show tracts commencing from the aortic root do not simply form an ascending segment, they also encircle the heart and on the contrary to the band make cross ventricular connections. The same applies for the bottom panels of Figure 10 (C,D), except that these tracts originate from the pulmonary root. These tracts encircle the pulmonary outflow tract, and furthermore cross to the left ventricle on the anterior surface of the heart, which again is conflicting to the description of the band.

The packing of cardiomyocytes and pump function

As with skeletal muscles, the matrix has endomysial and perimysial components. The endomysium forms the interconnected tubes in which the individual cardiomyocytes are strongly fixed by the struts

of the fibrous network (Anderson et al, 2009a). Throughout the ventricular walls, these endomysial bindings link together the cardiomyocytes into aggregates termed lamellar units. These heterogeneous aggregations have a long axis that follows the principle orientation of the cardiomyocytes. Their width and height is defined by the number of laterally and vertically connected myocytes respectively, as viewed in the short axis of the cardiomyocytes (Figs. 2-3). They are then separated by clefts lined by the perimysial component of the matrix. The perimysial components within the ventricular walls, however, are far less dense than those found in skeletal muscles. Unlike the situation in the skeletal muscles, the purpose of the perimysial clefts in the ventricular cone appears to be primarily to permit the lamellar units to move relative to one another during contraction and relaxation (LeGrice et al., 1995b) The perimysial component is not substantial enough to structurally and functionally compartmentalise regions of muscle, as is the case in skeletal muscle. In addition, the perimysial tissue keeps in register the branchings of the coronary arterial and venous systems, the lymphatic channels, and the nerves. As yet, we are unable to explain the differences in structure of the perimysium when comparing hearts of different species. In cattle heart, the perimysium is well formed, whereas in the porcine and rabbit hearts it is relatively tenuous.

It has long been known that the thickening of the ventricular walls seen during their systolic contraction cannot adequately be explained on the basis of the thickening of the individual cardiomyocytes alone (Spotnitz et al., 1974). Instead, during systole, there has to be gliding of the aggregated cardiomyocytes relative to one another (Anderson et al., 2008). It is the complex architecture and branching nature of the interconnected lamellar units within the walls that permits this regular realignment of the myocardial aggregates during systolic contraction and diastolic relaxation. A useful demonstration of the substructure of the ventricular walls may be made by distending the structure by injection of compressed air into the coronary arteries. The endomysial component of the connective tissue matrix is sufficient to preserve the lamellar architecture of the walls whereas the weaker perimysial components of the matrix are partially disrupted by the pneumatic distension, revealing the specific alignments and size of the lamellar units (Lunkenheimer and Niederer, 2012).

The results of such pneumatic distension have provided another difficulty for the proponents of the helical ventricular myocardial band. If the cardiomyocytes were truly aggregated together as suggested by Torrent-Guasp, then it might be expected that the band would be revealed by the pneumatic distension, showing its purported origin from the pulmonary trunk, and its insertion into the aorta. In contrast, the distension reveals a complex three-dimensional meshwork of myocyte aggregates with no separation into a band that spans the entire ventricular myocardium as suggested by Torrent Guasp. The overall alignment of the units is in keeping with the reciprocal helical patterns revealed by Pettigrew using gross dissections (Pettigrew, 1864), and by Streeter and Greenbaum, along with their respective colleagues, subsequent to histological investigations (Streeter and Bassett, 1966; Greenbaum et al., 1981). The patterns seen within a short axis view of the pneumatically distended ventricular cone are exactly as described by Feneis (1943) (Figs. 11-12), whose own findings endorsed the presence of a central band of circumferential cardiomyocytes as reported by Pettigrew and von Krehl (Feneis, 1943). There are, however, no physical anatomical boundaries to be found within the different components of the ventricular walls. It is possible to recognise five basic patterns, nonetheless, when tracing the aggregates of cardiomyocytes from the epicardium to the endocardium (Redmann et al., 2011). This will be discussed in the following section.

The "Feathering" of the Ventricular Mass

The outermost, subepicardial, component of the ventricular walls is made up of obliquely oriented cardiomyocytes that approach but do not reach vertical alignment with the long axis of the heart. This compact outer layer, barely distended by the pneumatic process, is thin when compared with the overall mural thickness (Fig. 12). Throughout the greater part of the ventricular cone, the cardiomyocytes gather themselves into a second layer, which has the appearance in transverse sections of half a feather (Figs. 11-12). The fronds of the feather, as they approach towards the middle of the ventricular wall, gradually approach a circumferential orientation, forming a central spine. From this central circumferential component, a separate array of lamellar units extends towards the endocardial lining of

the ventricular cavity, but extending in the opposite direction to the subepicardial half of the ‘feather’ (Figs. 11-12). Just before reaching the endocardium, the cardiomyocytes again become aggregated together in an almost longitudinal orientation, losing any obvious lamellar architecture, and producing another compact, and barely distended, fifth layer of the ventricular wall that includes the endocardial trabeculations (Fig. 12).

When traced in a long axis view, rather than a short axis view, the aggregates of myocytes making up the halves of the feathered arrangement extend in helical fashion throughout the length of the ventricular cone. Hence the “feathering” is strictly a 2-dimensional observation in the short-axis view, 3-dimensional representations of this arrangement would appear as a complex mesh as previously described (Lunkenheimer and Niederer, 2012; Redmann et al., 2011). It is impossible when using histological sections, however, to determine the extent and alignment of the aggregates themselves. It is likewise impossible, at present, to identify the dimensions of the aggregated units when using diffusion tensor magnetic resonance imaging, although such imaging does show clearly the average alignment of the long chains of cardiomyocytes, and predict the relative orientation of the lamellar units (Kung et al., 2011). The resolution of the technique, nonetheless, is currently insufficient to determine the detailed course of the cardiomyocytes within the tracts generated by the image-processing algorithms used to interpret the datasets. Unfortunately, such tracts have too often been interpreted as representing real fibrous structures within the ventricular mass.

Histological sections of distended myocardium reveal that the outermost subepicardial, along with the innermost subendocardial, layers of the walls are less obvious at the apex and base of the cone. At the apex, in particular, the spiralling lamellar units of the feather turn in opposing fashion, as was illustrated so long ago by Pettigrew (Pettigrew, 1864) and confirmed recently by Smerup and co-workers (Smerup et al., 2009). The sections also demonstrate that the spine of the feather, made up of cardiomyocytes aligned in circumferential fashion, changes its location within the depths of the wall along the length of the ventricular cone, and also varies in its own thickness. This circumferential central component, or

spine, furthermore, cannot be detected at the apex. It is also lacking at the very base of the ventricular cone. We believe that the use of micro-computed tomography will permit detection of the extent of the units into which the cardiomyocytes are aggregated. An example of a segmented aggregate is given in Figure 3. Figure 2 includes a histological section of a ventricular tissue preparation that was scanned with micro-computed tomography at 5 micron resolution after iodine enhancement. The 2-dimensional micro-computed tomography images illustrate that the lamellar units, and the individual cells which constitute them, are resolved by the technique. This 3-dimensional data contains sufficient information to extract the myocyte chains and their orientation. Although the perimysial space appears empty for the most part, our initial studies show that the lamellar units themselves form branches (see asterisks in Fig. 2) that communicate with neighbouring units, reinforcing the notion that the ventricular cone is a three-dimensional meshwork of interconnected cardiomyocytes (Lunkenheimer et al., 2006).

When considered relative to the entirety of the ventricular cone, therefore, the architecture of the lamellar units is remarkably complex, with each unit differing markedly in its size and alignment within the wall. The illustration from the Auckland group that illustrates the lamellar units extending in transmural fashion from epicardium to endocardium is thus an over-simplification (LeGrice et al., 1995a). Histological interrogation of hearts distended by pneumatic distension shows that, although separated by obvious perimysial clefts, there are multiple connections between the lamellar units, and this fact has been confirmed by our initial studies using micro-computed tomography (see asterisks in Fig. 2). Within each lamellar unit, there are then further endomysial connections between the individual cardiomyocytes. As emphasised above, therefore, the arrangement is one of a three-dimensional mesh, but with an obvious lamellar architecture. This notion of the three-dimensional alignment of lamellar units is entirely compatible with the images produced by the Auckland group using confocal microscopy (Pope et al., 2008). It is not, however, compatible with the notion that the ventricular cone is formed on the basis of a helical ventricular myocardial band of cardiomyocytes aligned in its long axis (Buckberg et al., 2005).

Significance to Muscular Dynamics

The differences between the anatomical arrangement of the cardiomyocytes, and their skeletal counterparts, reflect the dynamics of muscular contraction. Unlike skeletal muscles, the myocardium is not suspended between fixed points. Other than its external pericardial fixation within the mediastinum, the hearts lacks internal fixation. The shape, size, and limits of motion of the ventricular cone are determined only by its inner structure, and the contained mass of moving blood. Since ventricular activity itself is bi-phasic, consisting of systolic constriction and diastolic dilation, there must be two opposing impulses acting repetitively in two opposing directions. The discipline of classical cardiac physiology, for better or worse, had decided that diastolic ventricular unfolding and refilling are strictly passive, driven by venous filling pressure (Harvey, 1628). During the course of the twentieth century, nonetheless, it was proven that end-diastolic ventricular shape can be restored even at zero filling pressure (Gilbert and Glantz, 1989; Pieper and Martin, 1964). It was also shown that the ventricle is able to generate sub-atmospheric pressures when venous return is hampered (Brecher, 1958; Hori et al., 1982; Meesmann, 1958; Sabbah et al., 1981). It follows, therefore, that there must be active forces, which continue during diastole. We have shown that the structural substrate for the dilating forces, which act within the myocardial mass, is the non-tangential component of the three-dimensional myocardial mesh (Lunkenheimer et al., 2004). This population of cardiomyocytes, which are aligned in transmural fashion, are able to generate forces which act against systolic mural thickening. Up to two-fifths of the cardiomyocytes aggregated together with the ventricular cone lack a strictly tangential alignment, with the angulation of the non-tangential chains reaching values of intrusion and extrusion, respectively, of up to 40 degrees in diastole (Lunkenheimer at al., 2006). The values can exceed 45 degrees in systole, or in the hypertrophic heart (Smerup et al., 2013a; Smerup et al., 2013b). Direct measurements have been made of the local forces developed in the components of the mesh aligned in tangential and intruding fashion (Lunkenheimer et al., 2004). The population aligned in tangential fashion follows the prediction made by Laplace, namely that the peak force is reached in early systole, with a decline over the ejection period (LaPlace, 1805). These are unloading forces. The local forces

generated by the population of cardiomyocytes aligned in transmural or intruding fashion, in contrast, increase throughout the period of ejection, while acting against systolic wall thickening. The particular feature of these so-called auxotonic forces is that they are markedly more sensitive to inotropic interventions, in both positive and negative directions, than are the unloading type of forces. We suggest that this intrinsic antagonistic function drives early diastolic ventricular unfolding, provides the exact tuning of regional inward motion in terms of its amount and velocity, and controls ventricular tone. The combination of these effects is to control the intrinsic preload, that is, the end diastolic luminal volume, in other words, the initial stretching of the cardiomyocytes prior to contraction. Disregarding the transmural or intruding alignment of the cardiomyocytes, which we have demonstrated unequivocally using histological, diffusion tensor magnetic resonance imaging and micro-CT analysis (Figs. 5-6,12), as is the case with the helical ventricular myocardial band, is erroneous. Preparation of the band destroys these structures and thus disregards the functional implications of the antagonistic auxotonic forces they produce.

Conclusions

We have highlighted the similarities and differences with regards skeletal and cardiac muscle gross structure, tissue activation, connective tissue architecture, and cellular arrangement. Although both the skeletal and cardiac myocyte share the same functional unit, the sarcomere, cardiomyocytes are around 4 orders of magnitude smaller, and are electrically coupled to neighbouring cells via end-to-end connections and side branches. Skeletal and cardiac muscle share a hierarchical arrangement of connective tissue structures, namely they both have identifiable epimysium, perimysium and endomysium. Skeletal muscle has dense perimysial networks compartmentalising the muscle into distinct innervated bundles, or fascicles, of longitudinally aligned myocytes, which can be selectively activated. This is not the case for the ventricular myocardium. The less dense perimysial network, complex orientation of cardiomyocytes, and the heterogeneous lamellar units their aggregations form, make for a complex meshwork without distinct compartmentalisation. This means, generally speaking,

skeletal muscles produce force along the long axis of the muscle fibres. On the contrary, the complex myocardial meshwork produces lengthening, shortening, torsional, and antagonistic forces in multiple directions, and these forces have been shown to have both unloading and auxotonic characteristics.

Some investigators still maintain that the ventricular mass can be unwrapped in the form of a “helical ventricular myocardial band”. This implies that the muscle of the ventricular cone is arranged, comparable to that of skeletal muscles, in an ordered fashion, as a compartmentalised band of muscle with selective regional innervation and deformation, and a defined origin and insertion. In this review, we have shown that an understanding of the complex arrangement of cardiomyocytes within the walls of the heart requires not only knowledge of the muscle cells themselves, but also an appreciation of the precise manner of their packing within the supporting connective tissue matrix. We have shown how visualisation and segmentation of 3-dimensional image data can identify the morphology and orientation of the cardiomyocytes, and the lamellar units they form. In contrast to the simpler interpretation of the helical ventricular myocardial band, we provide insight as to how the complex myocytic chains, the heterogeneous lamellar units, and connective tissue matrix form an interconnected meshwork, which facilitates the complex internal deformations of the ventricular wall. We stress the dangers of disregarding the transmural or intruding alignment of the cardiomyocytes, as is the case with the helical ventricular myocardial band. Preparation of the band destroys these structures, and thus disregards the functional implications of the antagonistic auxotonic forces they produce. We conclude that the ventricular myocardial mass is a complex 3-dimensional meshwork with a higher order, heterogeneous and branching, lamellar architecture.

References

Abd-el-Malek S. 1939. Observations on the morphology of the human tongue. J Anat 73:201-210.203.

Anderson RH, Devine WA, Ho SY, Smith A, McKay R. 1991. The myth of the aortic annulus: The anatomy of the subaortic outflow tract. The Annals of Thoracic Surgery 52:640-646.

Anderson RH, Ho SY. 1998. The architecture of the sinus node, the atrioventricular conduction axis, and the internodal atrial myocardium. Journal Of Cardiovascular Electrophysiology 9:1233-1248.

Anderson RH, Sanchez-Quintana D, Niederer P, Lunkenheimer PP. 2008. Structural-functional correlates of the 3-dimensional arrangement of the myocytes making up the ventricular walls. The Journal of thoracic and cardiovascular surgery 136:10-18.

Anderson RH, Smerup M, Sanchez-Quintana D, Loukas M, Lunkenheimer PP. 2009a. The three-dimensional arrangement of the myocytes in the ventricular walls. Clinical Anatomy 22:64-76.

Anderson RH, Yanni J, Boyett MR, Chandler NJ, Dobrzynski H. 2009b. The anatomy of the cardiac conduction system. Clinical Anatomy 22:99-113.

Ansari A, Yen Ho S, Anderson RH. 1999. Distribution of the Purkinje fibres in the sheep heart. The Anatomical Record 254:92-97.

Arts T, Meerbaum S, RENEMAN RS, CORDAY E. 1984. Torsion of the left ventricle during the ejection phase in the intact dog. Cardiovascular Research 18:183-193.

Arts T, Reneman R, Veenstra P. 1979. A model of the mechanics of the left ventricle. Annals of Biomedical Engineering 7:299-318.

Aslanidi O, Nikolaidou T, Zhao J, Smaill B, Gilbert S, Jarvis J, Stephenson RS, Hancox J, Boyett M, Zhang H. 2012. Application of Micro-Computed Tomography with Iodine Staining to Cardiac Imaging, Segmentation and Computational Model Development. Medical Imaging, IEEE Transactions on PP:1-1.

Barnett V, Iaizzo PA. 2009. Cellular Myocytes. In: Handbook of Cardiac Anatomy, Physiology, and Devices: Humana Press. p 147-158.

Bojsen-Moller F, Tranum-Jensen J. 1972. Rabbit heart nodal tissue, sinuatrial ring bundle and atrioventricular connxions identified as a neuromuscular system. J Anat 112:367-382.

Borg TK, Caulfield JB. 1981. The collagen matrix of the heart. Fed Proc 40 2037-2041.

Brecher GA. 1958. Critical Review of Recent Work on Ventricular Diastolic Suction. Circulation Research 6:554-566.

Buckberg G, Hoffman JIE, Mahajan A, Saleh S, Coghlan C. 2008. Cardiac Mechanics Revisited: The Relationship of Cardiac Architecture to Ventricular Function. Circulation 118:2571-2587.

Buckberg GD. 2005. Architecture must document functional evidence to explain the living rhythm. European Journal of Cardio-Thoracic Surgery 27:202-209.

Carlsson M, Cain P, Holmqvist C, Stahlberg F, Lundback S, Arheden H. 2004. Total heart volume variation throughout the cardiac cycle in humans. American Journal of Physiology - Heart and Circulatory Physiology 287:H243-H250.

Chandler NJ, Greener ID, Tellez JO, Inada S, Musa H, Molenaar P, DiFrancesco D, Baruscotti M, Longhi R, Anderson RH, Billeter R, Sharma V, Sigg DC, Boyett MR, Dobrzynski H. 2009. Molecular Architecture of the Human Sinus Node: Insights Into the Function of the Cardiac Pacemaker. Circulation 119:1562-1575.

Dean JW, Ho SY, Rowland E, Mann J, Anderson RH. 1994. Clinical anatomy of the atrioventricular junctions. Journal of the American College of Cardiology 24:1725-1731.

Dobrzynski H, Anderson RH, Atkinson A, Borbas Z, D'Souza A, Fraser JF, Inada S, Logantha SJRJ, Monfredi O, Morris GM, Moorman AFM, Nikolaidou T, Schneider H, Szuts V, Temple IP, Yanni J, Boyett MR. 2013. Structure, function and clinical relevance of the cardiac

conduction system, including the atrioventricular ring and outflow tract tissues. Pharmacology & Therapeutics 139:260-288.
Dobrzynski H, Li J, Tellez J, Greener ID, Nikolski VP, Wright SE, Parson SH, Jones SA, Lancaster MK, Yamamoto M, Honjo H, Takagishi Y, Kodama I, Efimov IR, Billeter R, Boyett MR. 2005. Computer Three-Dimensional Reconstruction of the Sinoatrial Node. Circulation 111:846-854.
Egerbacher M, Weber H, Hauer S. 2000. Bones in the heart skeleton of the otter (Lutra lutra). J Anat 196:485-491.
Eliška O. 2006. Purkinje fibers of the Heart Conduction System *The History and Present Relevance of the Purkinje discoveries*. ČASOPIS LÉKAŘŮ ČESKÝCH, 145.
Feneis H. 1943. Das Gefüge des Herzmuskels bei Systole und Diastole. Morphologisches Jahrbuch 89:371-406.
Froeling M, Oudeman J, Strijkers GJ, Maas M, Drost MR, Nicolay K, Nederveen AJ. 2015. Muscle Changes Detected with Diffusion-Tensor Imaging after Long-Distance Running. Radiology 274:548-562.
Gilbert JC, Glantz SA. 1989. Determinants of left ventricular filling and of the diastolic pressure-volume relation. Circ Res 64:827-852.
Gilbert SH, Benoist D, Benson AP, White E, Tanner SF, Holden AV, Dobrzynski H, Bernus O, Radjenovic A. 2012a. Visualization and quantification of whole rat heart laminar structure using high-spatial resolution contrast-enhanced MRI. American Journal of Physiology - Heart and Circulatory Physiology 302:H287-H298.
Gilbert SH, Sands GB, LeGrice IJ, Smaill BH, Bernus O, Trew ML. 2012b. A framework for myoarchitecture analysis of high resolution cardiac MRI and comparison with diffusion Tensor MRI. In: Engineering in Medicine and Biology Society (EMBC), 2012 Annual International Conference of the IEEE. p 4063-4066.
Greenbaum RA, Ho SY, Gibson DG, Becker AE, Anderson RH. 1981. Left ventricular fibre architecture in man. British Heart Journal 45:248-263.
Haibo N, Castro SJ, Stephenson RS, Jarvis JC, Lowe T, Hart G, Boyett MR, Henggui Z. 2013. Extracting myofibre orientation from micro-CT images: An optimisation study. In: Computing in Cardiology Conference (CinC), 2013. p 823-826.
Harvey W. 1628. Exercitatio anatomica de motu cordis et sanguinis in animalibus. Frankfurt IV.
Hiraoka M, Sano T. 1976. Role of sinoatrial ring bundle in internodal conduction. Am J Physiol 231:319-325.
Holmes AA, Scollan DF, Winslow RL. 2000. Direct histological validation of diffusion tensor MRI in formaldehyde-fixed myocardium. Magnetic Resonance in Medicine 44:157-161.
Hori M, Yeliin El, Sonnenblick EH. 1982. Left ventricular diastolic suction as a mechanism of ventricular filling. Jpn Circ J 46:124-129.
Hsu EW, Muzikant AL, Matulevicius SA, Penland RC, Henriquez CS. 1998. Magnetic resonance myocardial fiber-orientation mapping with direct histological correlation. American Journal of Physiology - Heart and Circulatory Physiology 274:H1627-H1634.
Huijing PA. 1999. Muscle as a collagen fiber reinforced composite: a review of force transmission in muscle and whole limb. Journal of Biomechanics 32:329-345.
Ingels NBJ. 1997. Myocardial fiber architecture and left ventricular function. Technology and Health Care 5:45-52.
James TN. 1963. The connecting pathways between the sinus node and A-V node and between the right and the left atrium in the human heart. American Heart Journal 66:498-508.
James TN. 1965. Anatomy of the sinus node, AV node and os cordis of the beef heart. The Anatomical Record 153:361-371.
Jeffery NS, Stephenson RS, Gallagher JA, Jarvis JC, Cox PG. 2011. Micro-computed tomography with iodine staining resolves the arrangement of muscle fibres. Journal of Biomechanics 44:189-192.

Kier W, Smith K. 1985. Tongues, tentacles and trunks: the biomechanics of movement in muscular-hydrostats. Zool J Linnean Soc 83:307-324.
Kung GL, Nguyen TC, Itoh A, Skare S, Ingels NB, Miller DC, Ennis DB. 2011. The presence of two local myocardial sheet populations confirmed by diffusion tensor MRI and histological validation. Journal of Magnetic Resonance Imaging 34:1080-1091.
LaPlace PS. 1805. Traité de Mécanique Céleste. In. Paris Imprimeur - Libraire pour les Mathématiques.
LeGrice IJ, Smaill BH, Chai LZ, Edgar SG, Gavin JB, Hunter PJ. 1995a. Laminar structure of the heart: ventricular myocyte arrangement and connective tissue architecture in the dog. American Journal of Physiology - Heart and Circulatory Physiology 269:H571-H582.
LeGrice IJ, Takayama Y, Covell JW. 1995b. Transverse Shear Along Myocardial Cleavage Planes Provides a Mechanism for Normal Systolic Wall Thickening. Circulation Research 77:182-193.
Lehto H, Tirri R. 1980. Characterization of contractions in mechanically disaggregated myocardial cells from the rat. Acta Physiologica Scandinavica 110:385-389.
Lev M, Simkins CS. 1956. Architecture of the human ventricular myocardium, technique for study using a modification of the

Mall-MacCallum method. Lab Invest 5:396-409.
Li J, Greener ID, Inada S, Nikolski VP, Yamamoto M, Hancox JC, Zhang H, Billeter R, Efimov IR, Dobrzynski H, Boyett MR. 2008. Computer Three-Dimensional Reconstruction of the Atrioventricular Node. Circulation Research 102:975-985.
Liu J, Dobrzynski H, Yanni J, Boyett MR, Lei M. 2007. Organisation of the mouse sinoatrial node: structure and expression of HCN channels. Cardiovascular Research 73:729-738.
Lunkenheimer P, Niederer P, Sanchez-Quintana D, Murillo M, Smerup M. 2013. Models of Ventricular Structure and Function Reviewed for Clinical Cardiologists. Journal of Cardiovascular Translational Research 6:176-186.
Lunkenheimer PP, Niederer P. 2012. Hierarchy and inhomogeneity in the systematic structure of the mammalian myocardium: Towards a comprehensive view of cardiodynamics. Technol Health Care 20:423-434.
Lunkenheimer PP, Redmann K, Florek J, Fassnacht U, Cryer CW, WÃ¼bbeling F, Niederer P, Anderson RH. 2004. The forces generated within the musculature of the left ventricular wall. Heart 90:200-207.
Lunkenheimer PP, Redmann K, Kling N, Jiang X, Rothaus K, Cryer CW, Wübbeling F, Niederer P, Heitz PU, Yen Ho S, Anderson RH. 2006. Three-dimensional architecture of the left ventricular myocardium. The Anatomical Record Part A: Discoveries in Molecular, Cellular, and Evolutionary Biology 288A:565-578.
Mall FP. 1911. On the muscular architecture of the ventricles of the human heart. American Journal of Anatomy 11:211-266.
Meesmann W. 1958. Nachweis der diastolischen Sogwirkung der Herzkammern und deren Einfluss auf die intrakardialen Druckabläufe. Z Kreisl Forsch 47:534-551.
Pettigrew JB. 1864. On the Arrangement of the Muscular Fibres in the Ventricles of the Vertebrate Heart, with Physiological Remarks. Philosophical Transactions of the Royal Society of London 154:445-500.
Pieper HP, Martin BD. 1964. Experiments on ventricular filling. Cardiologica 45:100-116.
Pope AJ, Sands GB, Smaill BH, LeGrice IJ. 2008. Three-dimensional transmural organization of perimysial collagen in the heart. American Journal of Physiology - Heart and Circulatory Physiology 295:H1243-H1252.
Ramaswamy KS, Palmer ML, van der Meulen JH, Renoux A, Kostrominova TY, Michele DE, Faulkner JA. 2011. Lateral transmission of force is impaired in skeletal muscles of dystrophic mice and very old rats. The Journal of Physiology 589:1195-1208.

Redmann K, Lunkenheimer PP, Stöppeler S, Spiegel U, Smerup MH, Agger P, Niederer P, Weiss S, Batista RV. 2011. Pneumographic Imaging of Potential Cleavage Planes within the Ventricular Myocardium in Histology and Computed Tomography. Bulletin of the Georgian National Academy of Sciences 5:115-119.

Rodriguez EK, Hunter WC, Royce MJ, Leppo MK, Douglas AS, Weisman HF. 1992. A method to reconstruct myocardial sarcomere lengths and orientations at transmural sites in beating canine hearts. American Journal of Physiology - Heart and Circulatory Physiology 263:H293-H306.

Russold MF, Ramnarine I, Ashley Z, Sutherland H, Salmons S, Jarvis JC. 2010. Practical and Effective Stomal Sphincter Creation: Evaluation in Pigs. Diseases of the Colon & Rectum 53:467-474.

Sabbah HN, Anbe DT, Stein PD. 1981. Can the human right ventricle create a negative diastolic pressure suggestive of suction? Catheterization and Cardiovascular Diagnosis 7:259-267.

Sanchez-Quintana D, Pizarro G, LÃ³pez-MÃnguez JRn, Ho S, Cabrera JA. 2013. Standardized Review of Atrial Anatomy for Cardiac Electrophysiologists. Journal of Cardiovascular Translational Research 6:124-144.

Satoh H, Delbridge LM, Blatter LA, Bers DM. 1996. Surface:volume relationship in cardiac myocytes studied with confocal microscopy and membrane capacitance measurements: species-dependence and developmental effects. Biophysical Journal 70:1494-1504.

Schmid P, Lunkenheimer PP, Redmann K, Rothaus K, Jiang X, Cryer CW, Jaermann T, Niederer P, Boesiger P, Anderson RH. 2007. Statistical Analysis of the Angle of Intrusion of Porcine Ventricular Myocytes from Epicardium to Endocardium Using Diffusion Tensor Magnetic Resonance Imaging. The Anatomical Record: Advances in Integrative Anatomy and Evolutionary Biology 290:1413-1423.

Smerup M, Agger P, Nielsen EA, Ringgaard S, Pedersen M, Niederer P, Anderson RH, Lunkenheimer PP. 2013a. Regional and Epi- to Endocardial Differences in Transmural Angles of Left Ventricular Cardiomyocytes Measured in Ex Vivo Pig Hearts: Functional Implications. The Anatomical Record 296:1724-1734.

Smerup M, Nielsen E, Agger P, Frandsen J, Vestergaard-Poulsen P, Andersen J, Nyengaard J, Pedersen M, Ringgaard S, Hjortdal V, Lunkenheimer PP, Anderson RH. 2009. The Three-Dimensional Arrangement of the Myocytes Aggregated Together Within the Mammalian Ventricular Myocardium. The Anatomical Record: Advances in Integrative Anatomy and Evolutionary Biology 292:1-11.

Smerup M, Partridge J, Agger P, Ringgaard S, Pedersen M, Petersen S, Hasenkam JM, Niederer P, Lunkenheimer PP, Anderson RH. 2013b. A mathematical model of the mechanical link between shortening of the cardiomyocytes and systolic deformation of the left ventricular myocardium. Technology and Health Care 21:63-79.

Spotnitz HM, Spotnitz WD, Cottrell TS, Spiro D, Sonnenblick EH. 1974. Cellular basis for volume related wall thickness changes in the rat left ventricle. Journal of Molecular and Cellular Cardiology 6:317-331.

Stephenson RS, Boyett MR, Hart G, Nikolaidou T, Cai X, Corno AF, Alphonso N, Jeffery N, Jarvis JC. 2012. Contrast Enhanced Micro-Computed Tomography Resolves the 3-Dimensional Morphology of the Cardiac Conduction System in Mammalian Hearts. PLoS ONE 7:e35299.

Street SF. 1983. Lateral transmission of tension in frog myofibers: a myofibrillar network and transverse cytoskeletal connections are possible transmitters. J Cell Physiol 114:364-364.

Streeter DD, Bassett DL. 1966. An engineering analysis of myocardial fiber orientation in pig's left ventricle in systole. The Anatomical Record 155:503-511.

Streeter DD, Spotnitz HM, PATEL DP, ROSS J, SONNENBLICK EH. 1969. Fiber Orientation in the Canine Left Ventricle during Diastole and Systole. Circulation Research 24:339-347.

Tawara S. 2000. The conduction system of the Mammalian heart : an anatomico-histological study of the atrioventricular bundle and the purkinje fibers / S. Tawara ; foreword by L. Aschoff,

translated by Kozo Suma, Munehiro Shimada, preface by R. H Anderson: London : Imperial College Press, c2000.
Torrent-Guasp F. 1957. Anatomia funcional del corazón : la actividad ventricular diastólica y sistólica. Madrid: Paz Montalvo.
Torrent-Guasp F, Kocica MJ, Corno AF, Komeda M, Carreras-Costa F, Flotats A, Cosin-Aguillar J, Wen H. 2005. Towards new understanding of the heart structure and function. European Journal of Cardio-Thoracic Surgery 27:191-201.
Zhao J, Butters TD, Zhang H, Pullan AJ, LeGrice IJ, Sands GB, Smaill BH. 2012. An Image-Based Model of Atrial Muscular Architecture: Effects of Structural Anisotropy on Electrical Activation. Circulation: Arrhythmia and Electrophysiology 5:361-370.

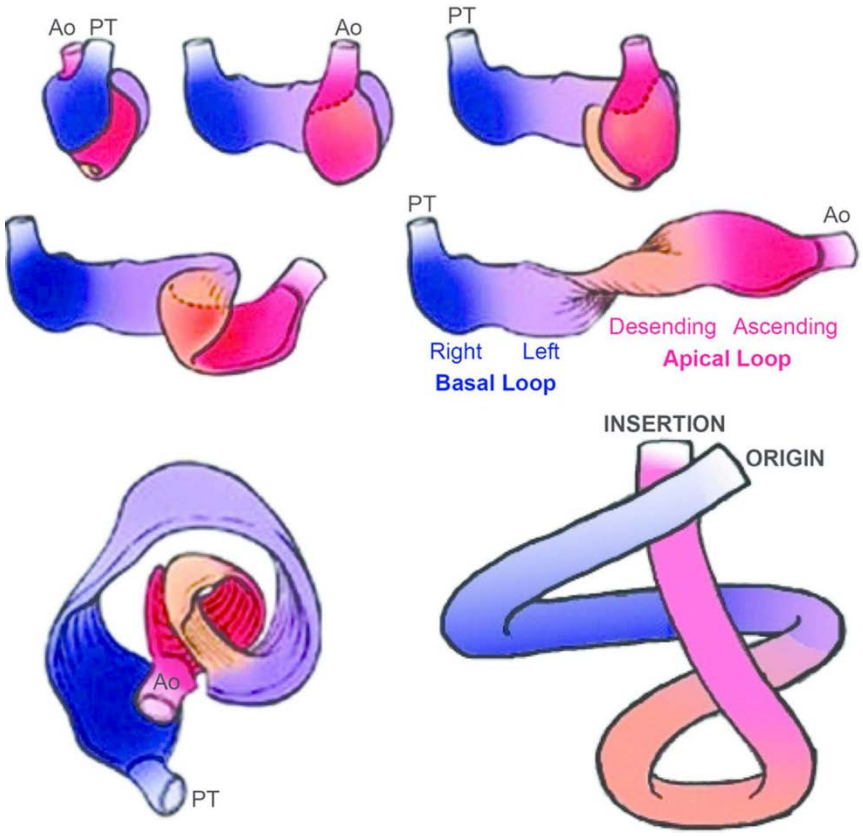

Figure 1. Schematic representation of the 'helical ventricular myocardial band', showing systematic unravelling of the band. Basal and apical loops indicated by blue and red colouration respectively, purported origin (pulmonary root) and insertion (aortic root) of the band are labelled. Ao- Aorta, PT- Pulmonary trunk.

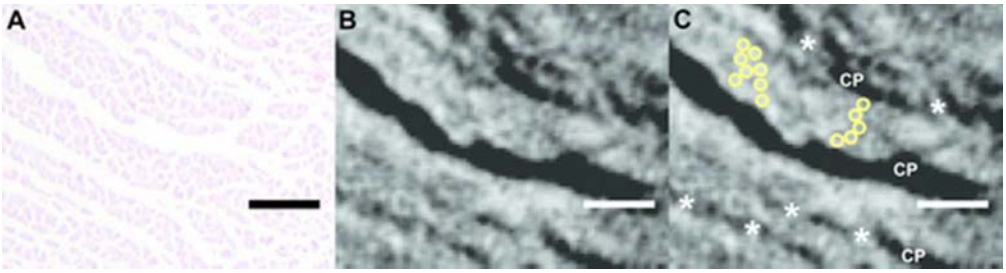

Figure 2 (A) Haematoxylin & Eosin stained longitudinal histological section of left ventricular posterior wall sample from rabbit (basal region). (B) Corresponding longitudinal micro-CT images, from the same sample as shown in panel A. (C) Reproduction of panel B indicating individual myocyte (yellow circles), inter- lamellar branches (*), and cleavage planes (CP). Scale bars represent 100 µm.

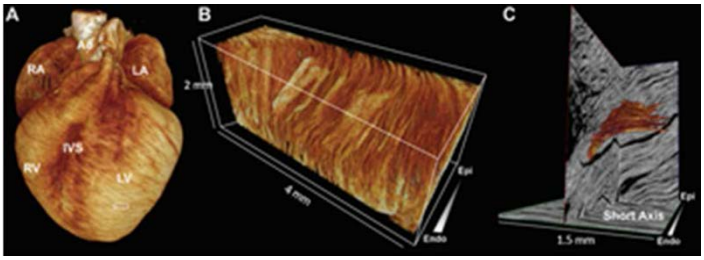

Figure 3 (D) Whole rabbit heart volume rendering derived from micro-CT data, showing region of interest presented in panel E (white box). (E) Volume rendering of subendocardial tissue block derived from dataset presented in D, showing the 3D morphology of multiple lamellar units. (F) Single lamellar unit (orange) segmented from micro-CT data of the rabbit left ventricular posterior wall, with individual myocyte chains resolved.

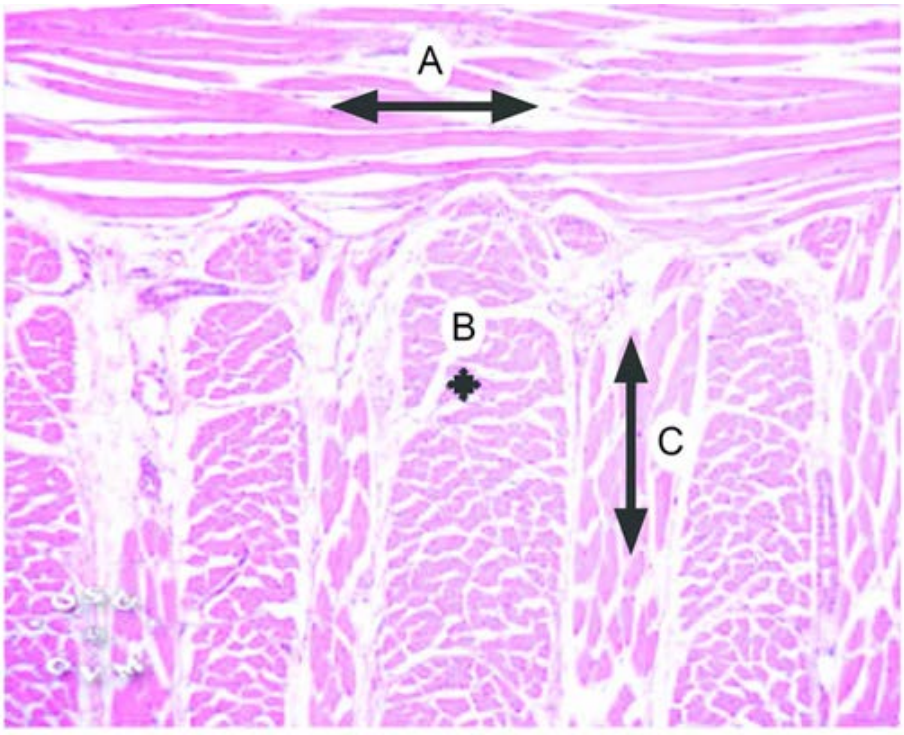

Figure 4 Haematoxylin & Eosin stained longitudinal histological section of a cat tongue, A indicates laterally running fibres, B indicates vertically running fibres, and C indicates individual myocyte cross sections. Image modified from https://instruction.cvhs.o kstate.edu/Histology/.

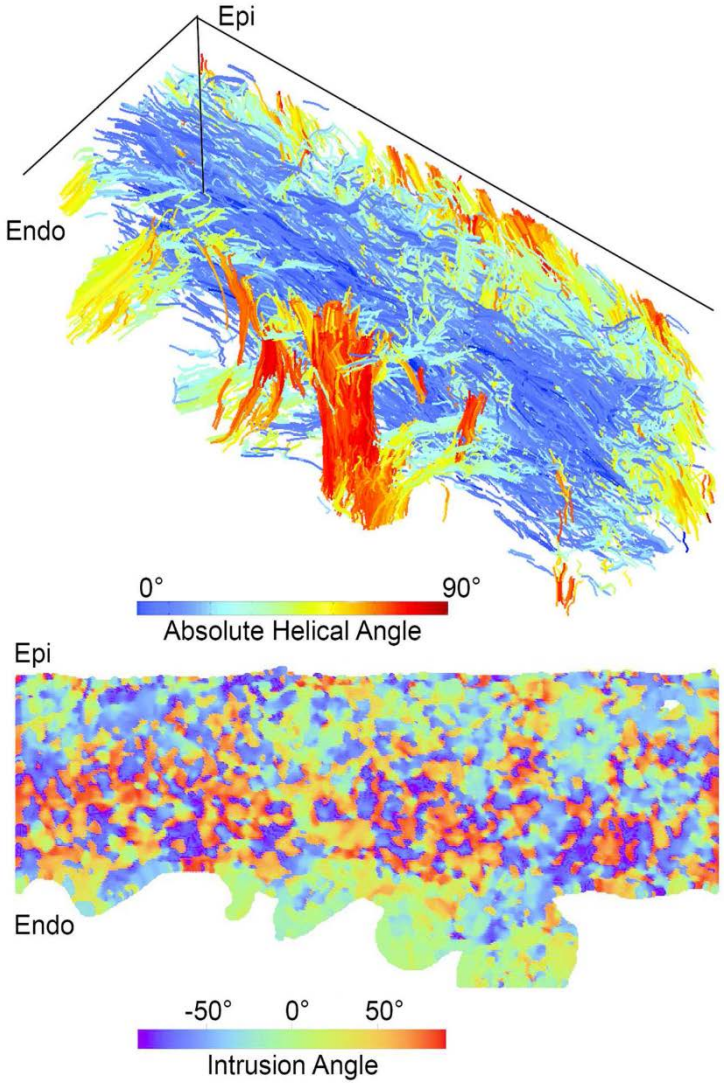

Figure 5 Three-dimensional myocyte helical angle colour map (top panel) of rabbit left ventricle posterior wall sample (~ 4 mm³), generated from eigen-analysis of micro-CT image data (spatial resolution 20 µm). Corresponding myocyte intrusion angle colour map of the centre z-axis slice (Lower panel)

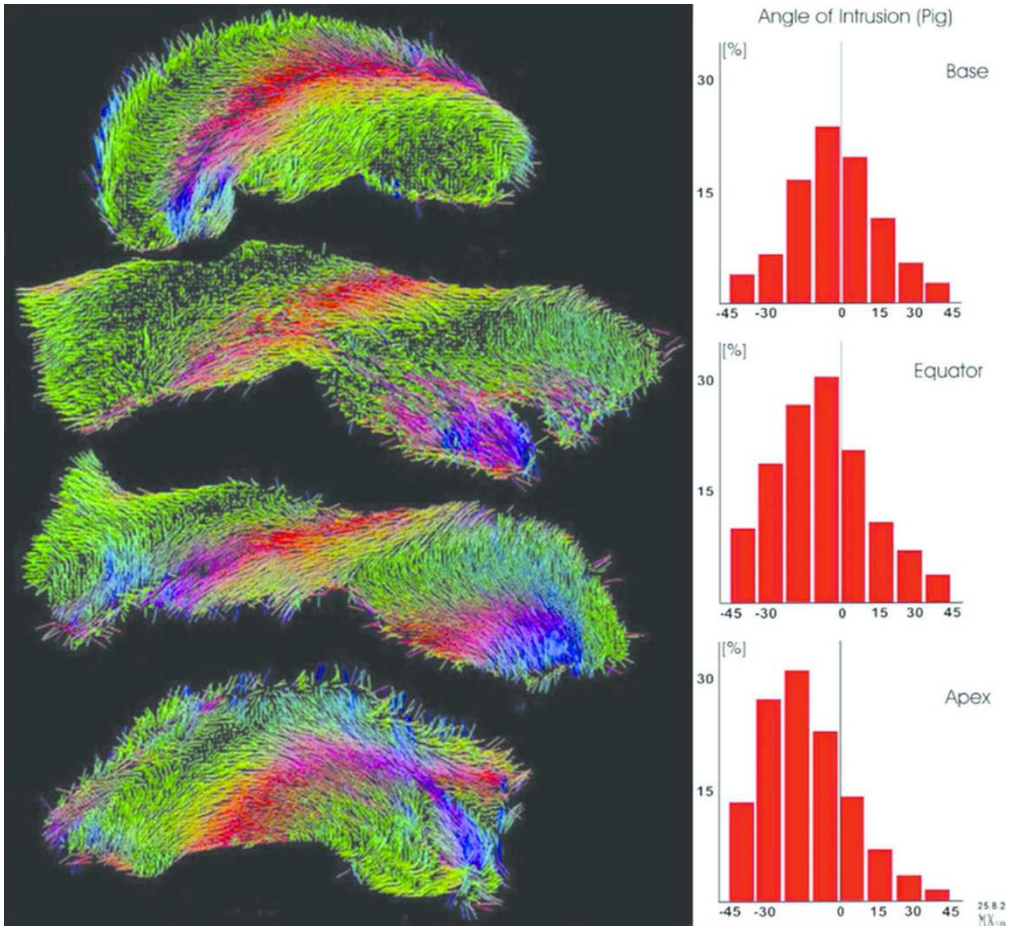

Figure 6 Diffusion tensor imaging tractography of porcine left ventricle harvested using circular knives; one basal, two equatorial, and one apical region are presented. The diagonal islands of longitudinally sectioned chains of myocytes are coloured red, with the other alignments coloured blue and green, the corresponding distribution of the intrusion angles of oblique structures are presented (modified from Lunkenheimer et al., 2013).

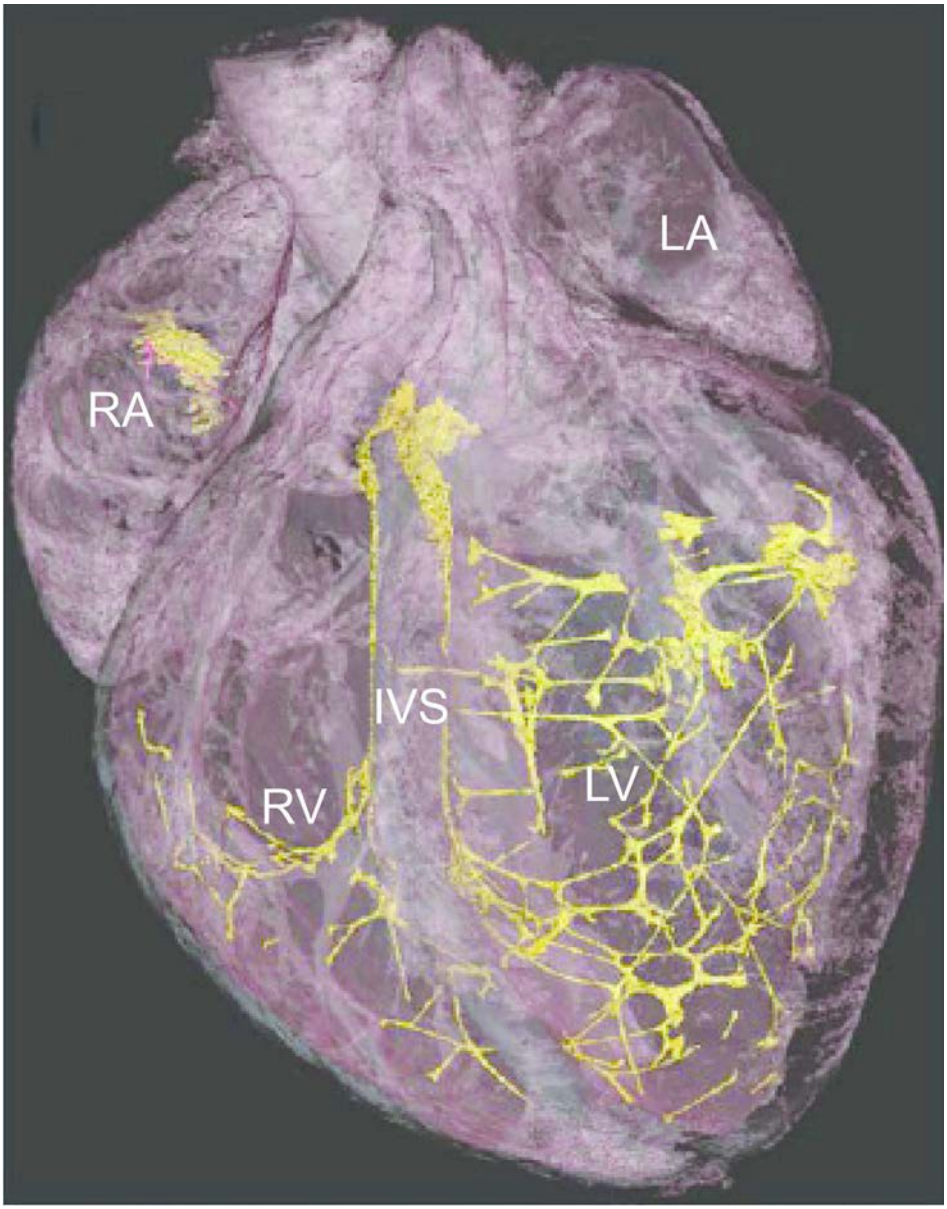

Figure 7 Whole rabbit heart segmentation of the cardiac conduction system (yellow), with ghosted myocardium overlaid (pink) (modified from Stephenson et al., 2012). IVS- interventricular septum, LA-left atrium, LV-left ventricle, RA-right atrium, RV-right ventricle.

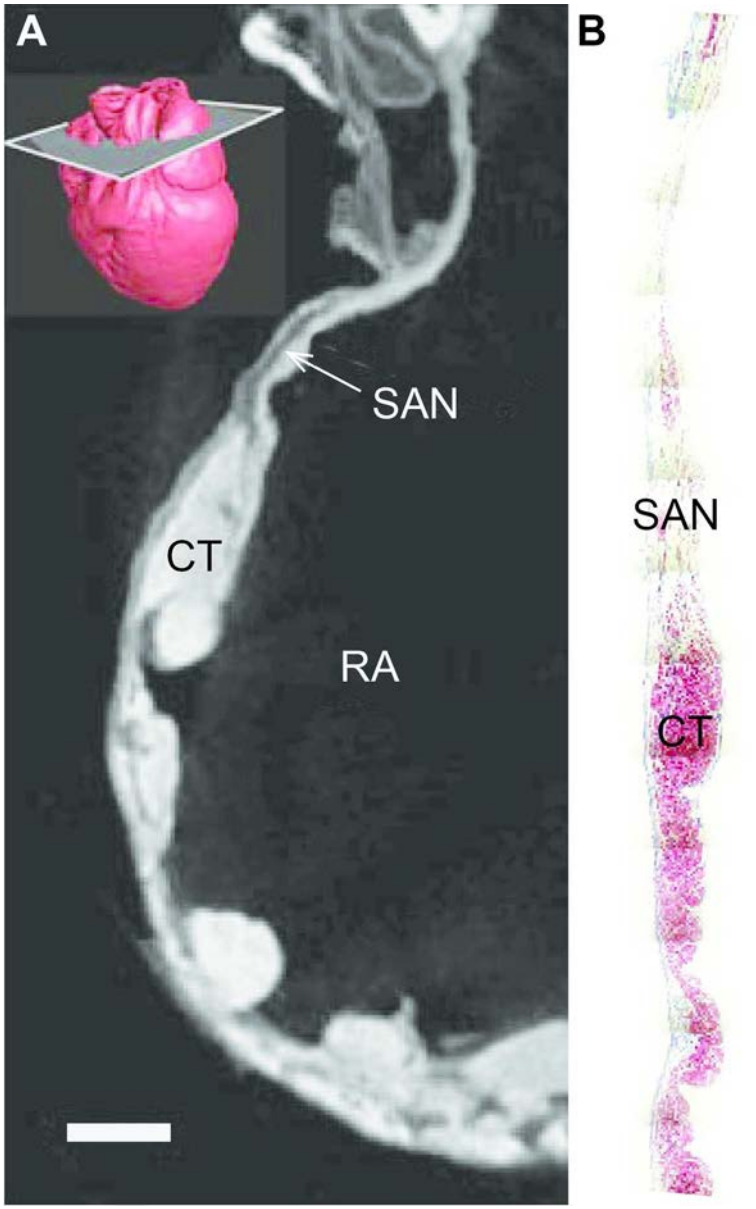

Figure 8 (A) Transverse micro-CT section of the posterior wall of the rabbit right atria, showing the location of the sinus node, plane of section with reference to the whole heart (top left) (modified from Stephenson et al., 2012), (B) corresponding Masson's trichrome stained histological section (modified from Dobrzynski et al., 2005). CT- cristae terminalis, RA- right atrium, SAN- sinus node. Scale bar represents 1000 µm.

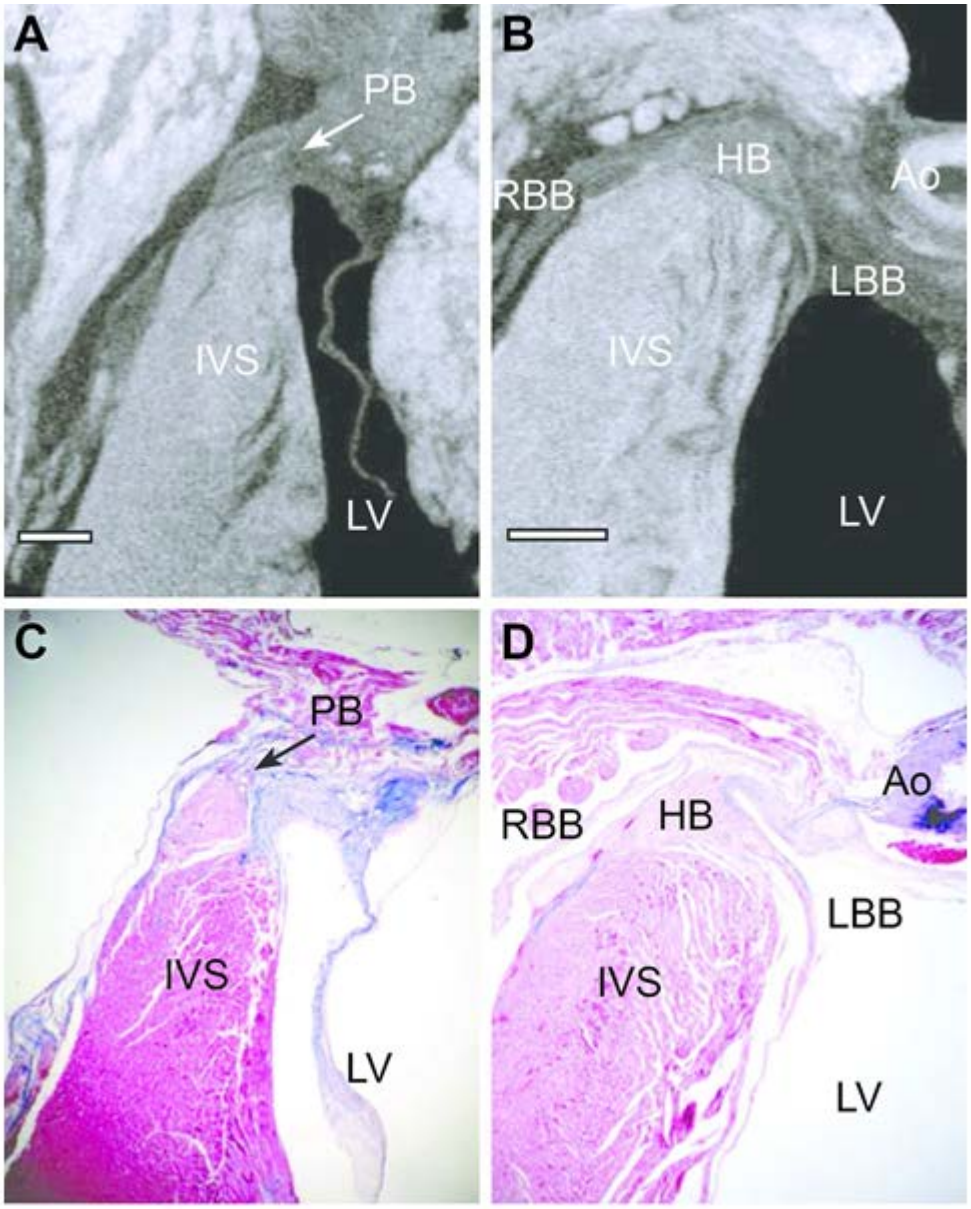

Figure 9 Longitudinal micro-CT section of the interventricular septum in the rabbit, showing the penetrating bundle (C) and anteriorly lying His bundle (E) as low attenuating structures (modified from Stephenson et al., 2012). Corresponding Masson's trichrome stained histological sections (D,F). AO- aorta, HB- His bundle, IVS- interventricular septum, LBB- left bundle branch, LV- Left ventricle, PB- penetrating bundle, RBB-right bundle branch. Scale bar represents 500 µm.

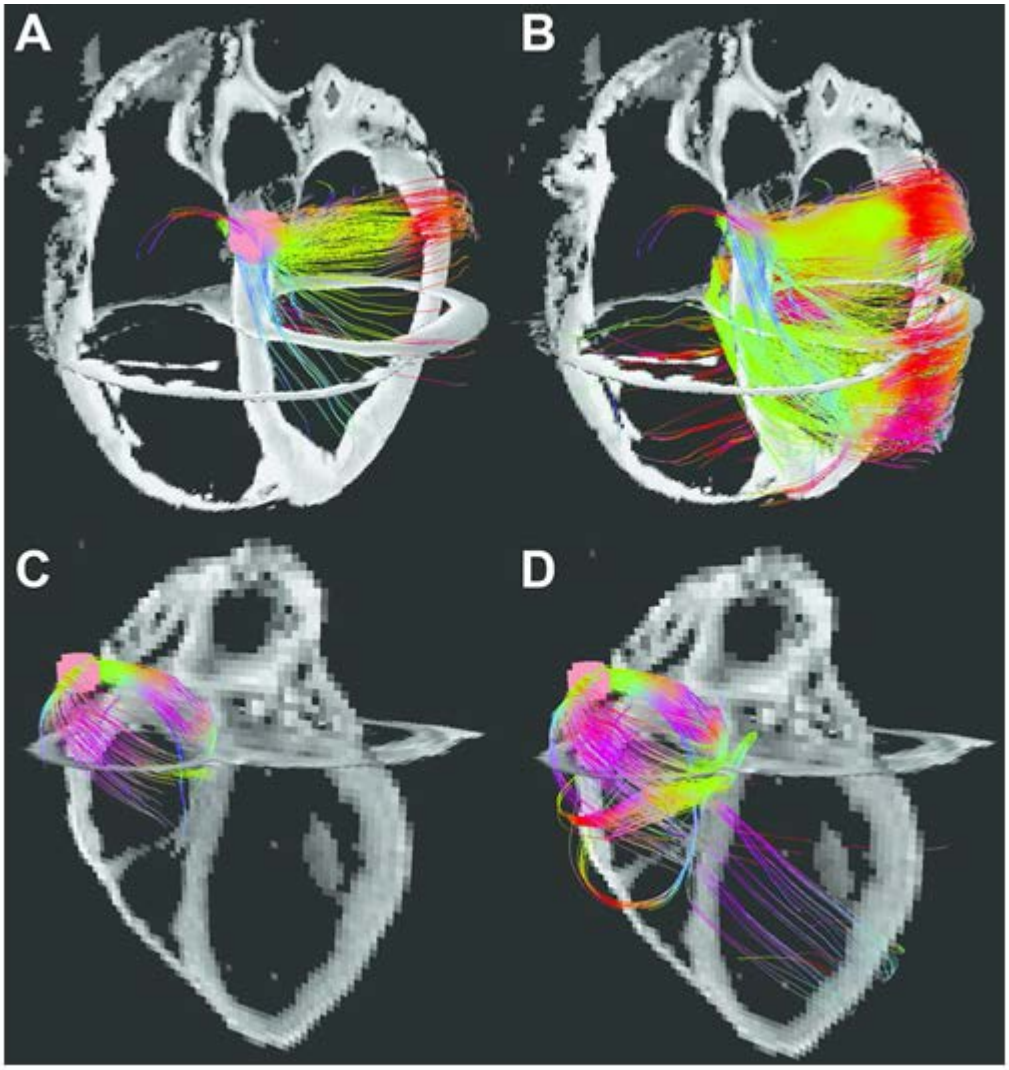

Figure 10 Diffusion tensor imaging tractography of the porcine heart, tractographies of increasing length originating from the basal septum near the aortic root (A, B), tractographies of increasing length originating from the pulmonary root (C, D). Colour coding of tracts is to aid visualisation and does not reflect tract angle.

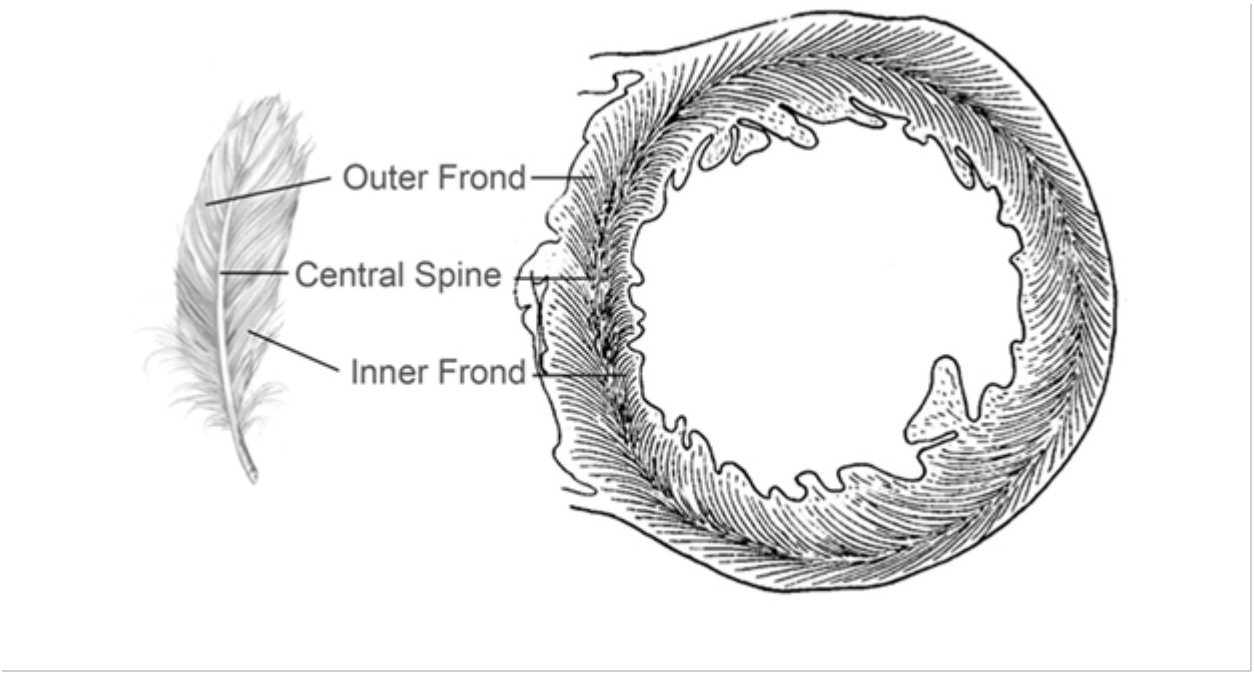

Figure 11 Schematic representation of myocardial feathering as viewed in the short-axis of the heart (modified from Feneis et al., 1943).

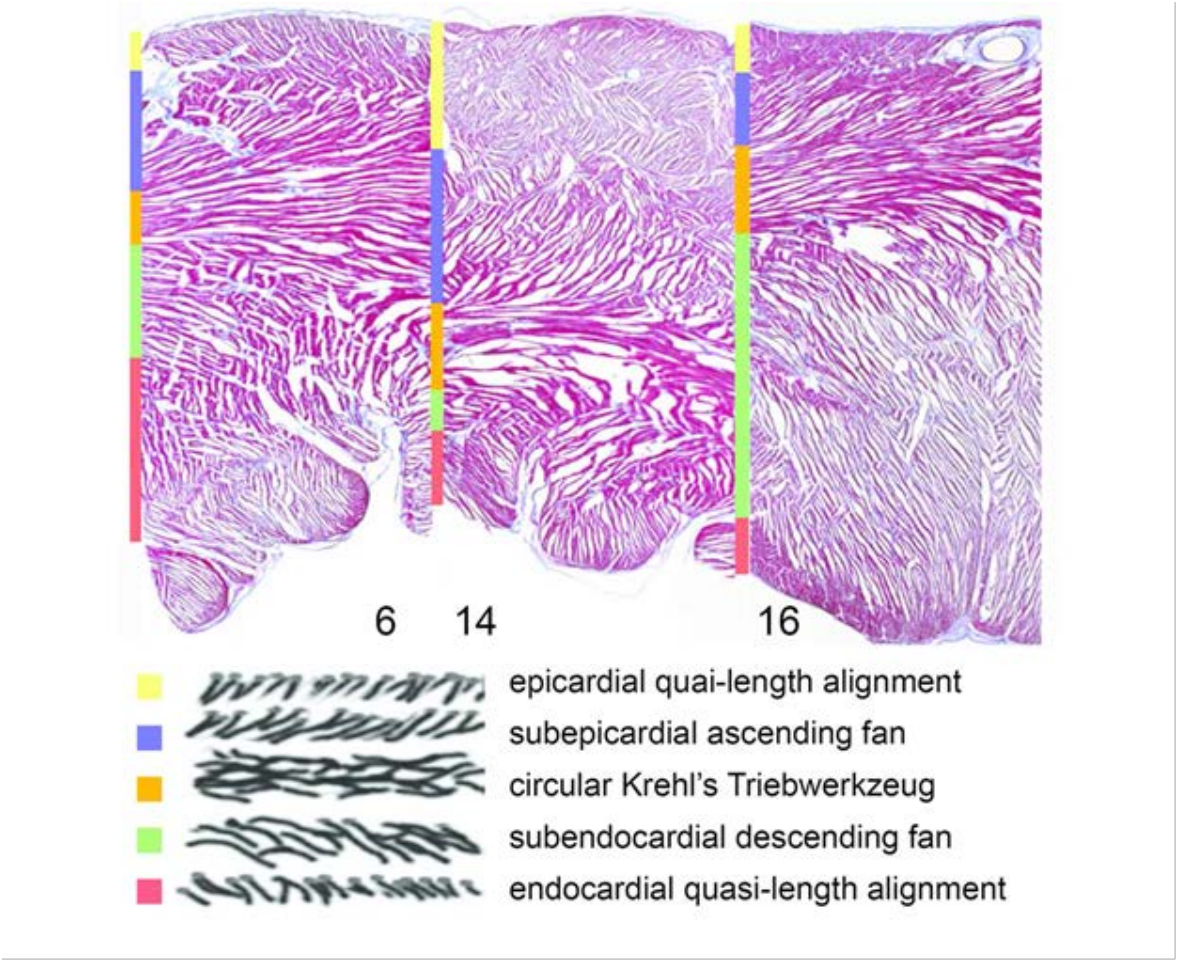

Figure 12 Azan stained short-axis histological section of the porcine heart (10x magnification) showing the typical feathered structure of left ventricular, cross sectioned at the base (area 6) and midway between base and equator (areas 14 and 16), with 5 arbitrarily discriminated layers. There are no demarcating connective tissue membranes between the "layers" (modified from Redmann et al., 2011).